

# Synthesis of Forsterite Powder from Zeolite Precursors

---

**Kosanović, Cleo; Stubičar, Nada; Tomašić, Nenad; Bermanec, Vladimir; Stubičar, Mirko; Ivanković, Hrvoje**

*Source / Izvornik:* **Croatica Chemica Acta, 2006, 79, 203 - 208**

**Journal article, Published version**

**Rad u časopisu, Objavljena verzija rada (izdavačev PDF)**

*Permanent link / Trajna poveznica:* <https://um.nsk.hr/um:nbn:hr:217:931295>

*Rights / Prava:* [Attribution 3.0 Unported](#)/[Imenovanje 3.0](#)

*Download date / Datum preuzimanja:* **2025-03-31**



*Repository / Repozitorij:*

[Repository of the Faculty of Science - University of Zagreb](#)



## Synthesis of Forsterite Powder from Zeolite Precursors

Cleo Kosanović,<sup>a,\*</sup> Nada Stubičar,<sup>b</sup> Nenad Tomašić,<sup>c</sup> Vladimir Bermanec,<sup>c</sup>  
Mirko Stubičar,<sup>d</sup> and Hrvoje Ivanković<sup>e</sup>

<sup>a</sup>Department of Material Chemistry, Ruđer Bošković Institute, Bijenička c. 54, 10000 Zagreb, Croatia

<sup>b</sup>Department of Chemistry, Faculty of Science, University of Zagreb, Marulićev trg 19/II, 10001 Zagreb, Croatia

<sup>c</sup>Institute of Mineralogy and Petrography, Faculty of Science, University of Zagreb, Horvatovac bb, 10000 Zagreb, Croatia

<sup>d</sup>Department of Physics, Faculty of Science, University of Zagreb, Bijenička c. 32, 10002 Zagreb, Croatia

<sup>e</sup>Department of Inorganic Chemical Technology and Non-metals, Faculty of Chemical Engineering and Technology, University of Zagreb, Marulićev trg 20, 10001 Zagreb, Croatia

RECEIVED APRIL 20, 2005; REVISED JULY 7, 2005; ACCEPTED JULY 13, 2005

**Keywords**  
ceramics  
forsterite  
zeolite precursor  
high energy ball-milling  
solid state transformation

Powder mixtures of NH<sub>4</sub>-exchanged zeolite A and MgO, and of NH<sub>4</sub>-exchanged mordenite and MgO were used as starting materials in the synthesis of crystalline ceramic materials. Conventional ball milling was applied in order to amorphize NH<sub>4</sub>-exchanged zeolites, reduce the particle size of MgO, and produce a homogeneous mixture. Solid-state transformation of the mixtures after heating at the temperature of their phase transformations in the interval 800 °C–1000 °C for 3 hours yielded crystalline forsterite (Mg<sub>2</sub>SiO<sub>4</sub>) with possible minor amounts of sapphirine (Mg<sub>4</sub>Al<sub>10</sub>Si<sub>2</sub>O<sub>23</sub>) in the first case, and to crystalline forsterite (Mg<sub>2</sub>SiO<sub>4</sub>) with traces of enstatite (MgSiO<sub>3</sub>) in the second case.

### INTRODUCTION

Forsterite is an end member of the olivine group of minerals named after the German scientist J. Forster. It consists of a pure magnesium silicate with the chemical formula Mg<sub>2</sub>SiO<sub>4</sub>. When the iron content increases over 50 %, it is named fayalite. Due to its high melting point and infusibility, withstanding temperatures of more than 1500 °C, the olivine group minerals are among the first to crystallize from magma. This is particularly useful in interpreting the origin of igneous rocks. The composition of the olivine in a given rock should reflect, to some extent, that of the parent magma. Forsterite is found in olivine of ultramafic igneous rocks highly enriched in

iron and magnesium (dunites and peridotites), many iron-nickel meteorites, and chondrite meteorites. The forsterite-fayalite solid solution series is sometimes used in the manufacture of refractory brick. Magnesium-rich olivine is unstable in a high-silica environment and is never found in equilibrium with quartz.

Like clinoenstatite (MgSiO<sub>3</sub>), synthetic forsterite has extremely low electrical conductivity.<sup>1,2</sup> This makes forsterite ceramics ideal substrate material for electronics. Due to its good refractoriness with the melting point at 1890 °C, excellent electrical insulation properties even at high temperatures, low dielectric permittivity, thermal expansion and chemical stability, forsterite is a material

\* Author to whom correspondence should be addressed. (E-mail: cleo@rudjer.irb.hr)

of interest to engineers and designers, especially as an active medium for tunable laser.<sup>3–5</sup> It is also of interest to the SOFC (Solid Oxide Fuel Cells) manufacturers because of its thermal expansion properties and chemical stability.

Forsterite has been synthesized by solid-state reaction between MgO and SiO<sub>2</sub>,<sup>6</sup> or bauxite and MgCO<sub>3</sub>,<sup>7</sup> but also by various sol-gel methods,<sup>2,8,9</sup> which include a H<sub>2</sub>O<sub>2</sub>-assisted process.<sup>10</sup> Forsterite whiskers were obtained by an oxidation-reduction reaction at 1500 °C using starting materials such as graphite, MgO, Al, and SiC.<sup>11</sup>

The aim of this study is to investigate the synthesis of crystalline forsterite using different zeolite precursors previously activated by ball milling. Use of zeolites as precursors has been chosen because of their uniform and narrow particle size distribution that enables a better control over the microstructure of the resulting ceramic phase.

NH<sub>4</sub>-exchanged zeolite A and NH<sub>4</sub>-exchanged synthetic mordenite are used as starting materials because a) of the suitable ratio of SiO<sub>2</sub>/Al<sub>2</sub>O<sub>3</sub> oxides in their composition, which results in a different percentage of forsterite phase in the product, b) they are easy to prepare and are also easy to provide commercially, c) using the ion exchange ability of zeolites, it is easy to eliminate sodium cations and convert them to the NH<sub>4</sub>-form of zeolite, which is much more suitable for thermal transformation (NH<sub>3</sub> is removed as a gas leaving a clear composition consisting of Al and Si in desired amounts), and finally d) they are inexpensive.

In this research, the solid-state phase transformations were observed at temperatures below 1000 °C.

## EXPERIMENTAL

Zeolite Linde 4A ([Na<sub>2</sub>O · Al<sub>2</sub>O<sub>3</sub> · 1.98SiO<sub>2</sub> · 2.12H<sub>2</sub>O]), synthesized by a known procedure<sup>12</sup> in our laboratory, and synthetic mordenite ([Na<sub>2</sub>O · Al<sub>2</sub>O<sub>3</sub> · 8.7SiO<sub>2</sub> · 7.24H<sub>2</sub>O]), a product of Union carbide Corp., were used as starting materials. Ion-exchange of the original Na<sup>+</sup> ions from the zeolite was carried out by a previously described procedure.<sup>13,14</sup> MgO was a product of Ventron with 99.5 % purity. X-ray diffraction analysis identified it as periclase (MgO) (Ref. 15; PDF 43-1022) and brucite (Mg(OH)<sub>2</sub>) (Ref. 15; PDF 44-1482).

A mixture of NH<sub>4</sub>-exchanged zeolite A and MgO in a mass ratio 1:0.15, and a mixture of NH<sub>4</sub>-exchanged synthetic mordenite and MgO in a mass ratio 1:1, were mechanically treated in a planetary ball mill (Fritsch Pulverisette type 7). A certain amount of the mixture was put in an agate vessel containing 10 agate balls ( $\phi = 10$  mm) and 4 agate balls ( $\phi = 12$  mm), and then milled for a predetermined time,  $t_m$  (10 min, 1 h, 3 h, 5 h, 6 h and 10 h).

The samples collected after 5 h (for the mixture of NH<sub>4</sub>-exchanged zeolite A and MgO) and 10 h (for the mixture of NH<sub>4</sub>-exchanged synthetic mordenite and MgO) of milling were heated in a chamber furnace with controlled tem-

perature (ELPH –2, Elektrosanitarij) at the temperature obtained by thermal analysis as the exothermic peak in the DSC curves. The samples were heated isothermally at an appropriate temperature for 3 h.

Starting materials, the milled and the subsequently post-annealed samples were characterized as follows.

XRD patterns of the samples were obtained on a Philips X'Pert PRO X-ray diffractometer using Cu-K $\alpha$  radiation. Powder diffraction data were collected in the range from 4° to 63° 2 $\theta$ , with the step size of 0.02°. The obtained  $d$ -spacing and the relative intensities of the X-ray diffraction lines were compared with the reported literature values.<sup>15</sup>

Infrared transmission spectra of the solid samples were obtained with the KBr wafer technique. The spectra were recorded using a FT-IR spectrometer System 2000 FT-IR (Perkin-Elmer) in the region from 400 to 4000 cm<sup>-1</sup> (20 scans).

Thermal analysis (DSC, differential scanning calorimetry and TG, thermogravimetry) of the sample obtained after 5 h and 10 h of milling was performed by a Netzch STA 409 simultaneous thermal analysis apparatus under a constant air flow of 30 cm<sup>3</sup> min<sup>-1</sup>. Platinum crucibles and alumina were used as a reference. The heating rate was 10 K min<sup>-1</sup>.

## RESULTS AND DISCUSSION

In order to obtain a homogeneous mixture before the thermal treatment, the starting materials were treated in a high-energy ball mill. IR spectra show that zeolite was completely amorphized after 5 h of milling in the case of NH<sub>4</sub>-exchanged zeolite A (Figure 1), and after 10 h in the case of NH<sub>4</sub>-exchanged synthetic mordenite (Figure 2). The ball milling of MgO, in both cases, resulted in a type I amorphization, which means that the amorphization is caused by the lowering of the crystallite size only.<sup>16</sup>

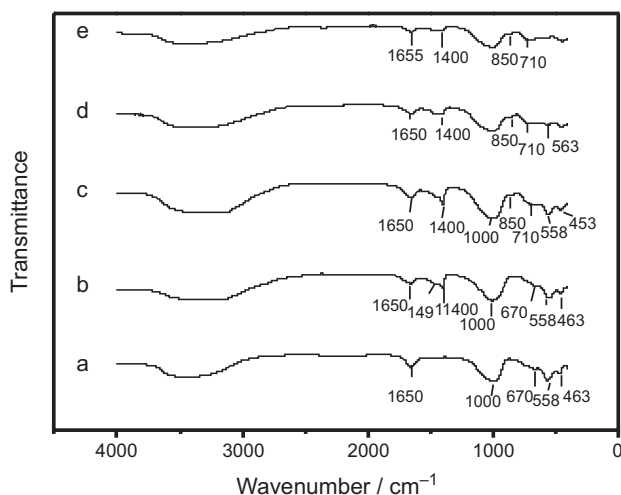


Figure 1. Infrared transmission spectra of NH<sub>4</sub>-exchanged zeolite A (a) and of the samples obtained by ball milling of the mixture of NH<sub>4</sub>-exchanged zeolite A and MgO in a ratio 1:0.15 for 10 min (b), 1 h (c), 3 h (d), and 5 h (e).

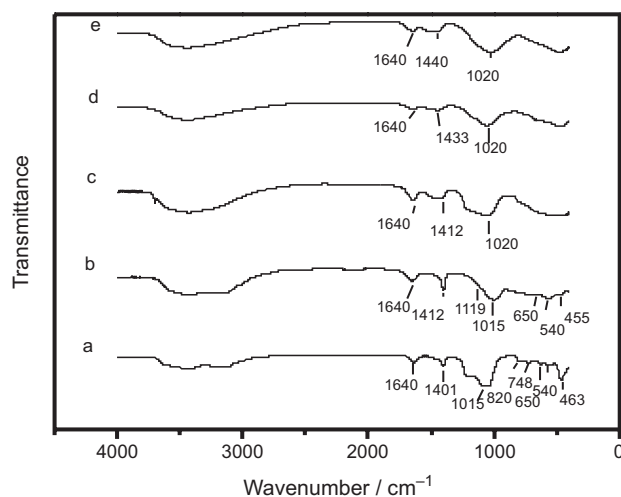


Figure 2. Infrared transmission spectra of  $\text{NH}_4$ -synthetic mordenite (a) and of the samples obtained by ball milling of the mixture of  $\text{NH}_4$ -synthetic mordenite and  $\text{MgO}$  in a ratio 1:1 for 10 min (b), 1 h (c), 3 h (d), and 10 h (e).

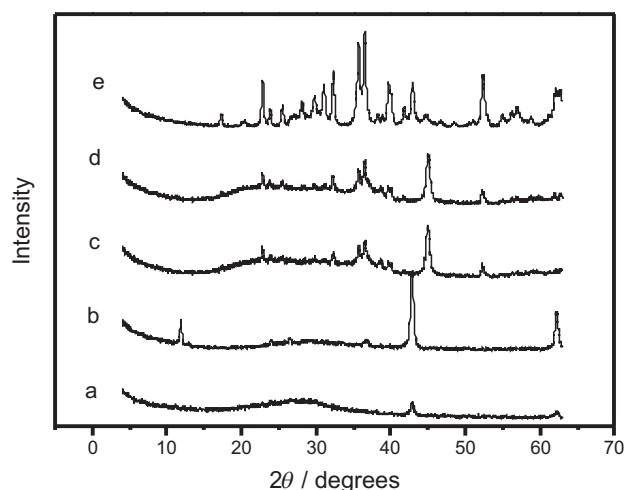


Figure 3. Series of the representative powder patterns of the samples: the mixture of  $\text{NH}_4$ -exchanged zeolite A and  $\text{MgO}$  in a ratio 1:0.15 (a), and the mixture of  $\text{NH}_4$ -synthetic mordenite and  $\text{MgO}$  in a ratio 1:1 (b) obtained after ball milling for 5 h and 10 h, respectively. Patterns (c) and (d) were obtained after heat treatment of sample (a) at 918 °C (c) and 974 °C (d), and (e) was obtained after sample heating (b) at 855 °C.

After 6 h of milling,  $\text{MgO}$  retains its crystallinity, reducing the particle size (Figure 3).

The IR spectrum of the starting  $\text{NH}_4$ -exchanged zeolite A powder in the mixture contains all the characteristic bands of zeolite A: the broad band at 1000  $\text{cm}^{-1}$  assigned to asymmetric stretching mode, the weak band at 670  $\text{cm}^{-1}$  assigned to symmetric stretching mode, the intense band at 558  $\text{cm}^{-1}$  assigned to external vibrations related to D-4 rings, and the band at 463  $\text{cm}^{-1}$  assigned to T-O bending (see spectrum a, Figure 1).<sup>16,17</sup> Loss of crystallinity is accompanied by a decrease of the band at 558  $\text{cm}^{-1}$ , and its shifting to 563  $\text{cm}^{-1}$ . Also, the weak band at 670  $\text{cm}^{-1}$  disappears and a new broad band at

710  $\text{cm}^{-1}$  and a shoulder at 850  $\text{cm}^{-1}$  appear (see spectra c, d and e, Figure 1). Changes of the IR spectra lead to the conclusion that the long-range ordering of the Si and Al atoms of the crystal framework of zeolite was transformed to short-range ordering, and the amorphization of zeolite was caused by the breaking of "external" Si-O-Si and Si-O-Al bonds of the zeolite framework structure. Amorphization of the  $\text{NH}_4$ -exchanged zeolite A follows the type II amorphization, which means it is caused by structural changes on the molecular level and not by the lowering of the crystal size below the X-ray detection limit. Amorphization by ball milling was completed after 5 h (see spectra e, Figure 1). The bands at 455  $\text{cm}^{-1}$ , 1400  $\text{cm}^{-1}$  and 1491  $\text{cm}^{-1}$  belong to  $\text{MgO}$ . As the particle size of  $\text{MgO}$  is decreasing, the band at 1491  $\text{cm}^{-1}$  disappears and the bands at 1400 and 1650  $\text{cm}^{-1}$  are shifted to 1410 and 1655  $\text{cm}^{-1}$ .

Similar results are obtained by the evaluation of the changes in the IR-spectra of the second starting material, the mixture of  $\text{NH}_4$ -exchanged synthetic mordenite and  $\text{MgO}$  caused by ball milling (see Figure 2).  $\text{NH}_4$ -exchanged synthetic mordenite progressively loses its crystallinity as a function of milling time,  $t_m$ , and is completely transformed to an amorphous phase after 10 h of a mechanical action. The longer time needed for complete amorphization of synthetic mordenite than for full amorphization of  $\text{NH}_4$ -exchanged zeolite A can be explained by the higher stability of 5-1 SBU in  $\text{NH}_4$ -exchanged synthetic mordenite<sup>18</sup> compared to the stability of D-4 and D-6 SBU in  $\text{NH}_4$ -exchanged zeolite A, as well as by the higher Si/Al ratio in  $\text{NH}_4$ -exchanged synthetic mordenite (Si/Al  $\cong$  5) than in  $\text{NH}_4$ -exchanged zeolite A (Si/Al = 1).<sup>19</sup> The strongest vibration at 1015  $\text{cm}^{-1}$  is assigned to a T-O stretch, involving motion probably associated with the oxygen atom. The next strongest band at 463 is assigned to a T-O bending mode. Stretching modes are assigned in the region of 650–820  $\text{cm}^{-1}$ . The band at about 650  $\text{cm}^{-1}$  corresponds to the symmetric stretching of T-O bonds. The most significant change in the amorphization of synthetic mordenite is the decreasing of the bands characteristic of the crystal structure of synthetic mordenite,<sup>17</sup> *i.e.*, the band at 540  $\text{cm}^{-1}$  characteristic of the 5–1 secondary building units (SBU) and the band at 650  $\text{cm}^{-1}$ .

X-ray powder diffractograms presented in Figure 3 show mixtures of  $\text{NH}_4$ -exchanged zeolite A and  $\text{MgO}$  (a), and of  $\text{NH}_4$ -exchanged synthetic mordenite and  $\text{MgO}$  (d) to have one characteristic amorphous halo after ball milling treatment. This indicates amorphization of zeolite and two wide peaks at 43 and 62  $2\theta^\circ$  belong to  $\text{MgO}$ .

The DSC curve of  $\text{NH}_4$ -exchanged zeolite A and  $\text{MgO}$  mixture after 5 h of ball milling (Figure 4A, a) is characterized by an endothermic peak at 100 °C < T < 200 °C caused by loss of water from the mixture. The endothermic peak at about 260 °C is accompanied by decomposition of the  $\text{NH}_4^+$  cation and removal of  $\text{NH}_3$  gas. The three

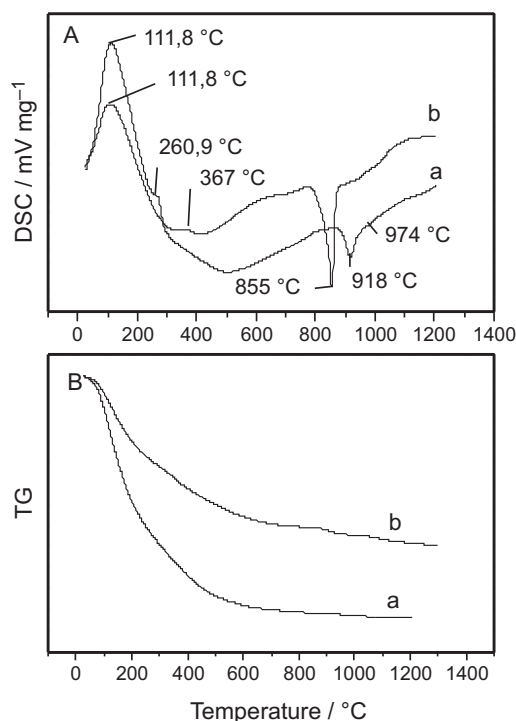


Figure 4. DSC (A) and TG (B) curves of the mixture of  $\text{NH}_4$ -exchanged zeolite A and MgO ball-milled for 5 h (a), and of the mixture of  $\text{NH}_4$ -synthetic mordenite and MgO ball-milled for 10 h (b).

exothermic peaks at temperatures of 918, 947, 974 °C are related to the phase transformation of the mixture to forsterite and minor amounts of other phases. DSC curve of  $\text{NH}_4$ -exchanged synthetic mordenite and MgO mixture after 10 h of ball milling (Figure 4A, b) shows an endothermic peak at 111 °C caused by water loss from the mixture. The endothermic peak at about 367 °C is related to decomposition of the  $\text{NH}_4^+$  cation and removal of  $\text{NH}_3$  gas as well as removal of the zeolitic water. The exothermic peak at the temperature of 855 °C is caused by the phase transformation of the mixture to forsterite and minor amounts of enstatite. The weight loss (Figure 4B, a, b) is given for both mixtures.

Thermal treatment of both investigated mixtures at temperatures of the exothermic peaks in DSC curves allows formulation of ceramic materials suitable for various engineering applications.

X-ray diffraction patterns (Figure 3 b, c, Figure 5 a) and IR spectra (Figure 6 a, b) for  $\text{NH}_4$ -exchanged zeolite A and MgO mixture show that, at both temperatures of the corresponding exothermic peaks, a mixture of forsterite and an amorphous phase is obtained. Additionally, the spinel ( $\text{MgAl}_2\text{O}_4$ ) phase and / or sapphirine might be present.

Diffraction patterns of the samples treated at 918 °C (Figure 3 b) and 974 °C (Figure 3 c, Figure 5 a in detail) exhibit halos superimposed by sharp reflections corresponding to crystalline forsterite [PDF 34-0189] (Ref. 14), and possibly spinel [PDF 21-1152] and sapphirine phase

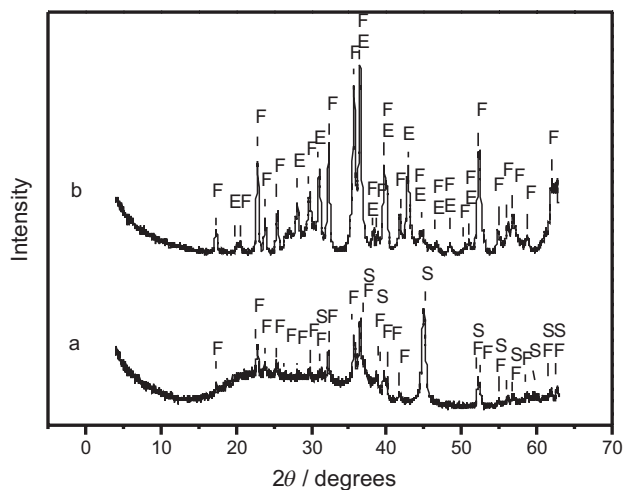


Figure 5. Diffractograms of the products obtained after calcinating the milled mixture of  $\text{NH}_4$ -exchanged zeolite A and MgO at 974 °C (a), and the milled mixture of  $\text{NH}_4$ -synthetic mordenite and MgO at 855 °C (b). The letters in patterns a) and b) indicate the angular positions of XRD peaks belonging to various crystalline phases likely to appear in the treated samples. F for forsterite, E for enstatite, and S for sapphirine.

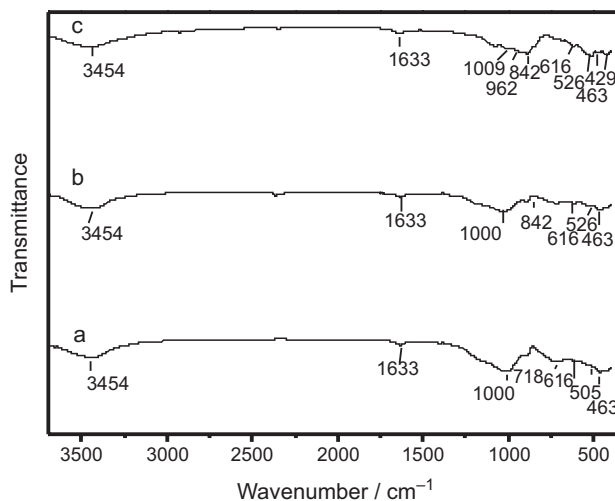


Figure 6. Infrared transmission spectra of the mixture of  $\text{NH}_4$ -exchanged zeolite A and MgO ball-milled for 5 h and heated at 918 °C (a) and (974 °C) (b), and of the mixture of  $\text{NH}_4$ -synthetic mordenite and MgO ball-milled for 10 h and heated at 855 °C (c).

[PDF 11-0607] (Ref. 14). Two intensive amorphous halos at 22.85 and 30.25  $2\theta^\circ$  differ from the diffraction pattern of amorphous  $\text{SiO}_2$  with one halo. It may be concluded that at least two amorphous phases coexist. Taking into consideration the stoichiometrics of the reaction mixture, two possible combinations of the amorphous phases could exist: amorphous phases related to  $\text{SiO}_2$  and forsterite, which have not crystallized yet or amorphous mullite ( $3\text{Al}_2\text{O}_3 \cdot 2\text{SiO}_2$ ) and  $\text{SiO}_2$ . Comparing the halos of the samples in Figure 4 with the known data obtained for the amorphous phases of  $\text{SiO}_2$  and mullite,<sup>20</sup> it may be concluded that the amorphous phase is a mixture of ( $3\text{Al}_2\text{O}_3 \cdot 2\text{SiO}_2$ ) and  $\text{SiO}_2$ .



The X-ray diffractogram (Figure 3 d, Figure 5 b in detail) obtained for the mixture of  $\text{NH}_4$ -exchanged synthetic mordenite and MgO calcined at 855 °C shows that the product is forsterite ( $\text{Mg}_2\text{SiO}_4$ ) [Ref. 15; PDF 32–0189] and traces of enstatite ( $\text{MgSiO}_3$ ) [Ref. 15; PDF 07–0216]. Due to the lower content of aluminum in the synthetic mordenite composition, additional phases like spinel or sapphirine are not obtained.

FT-IR spectra (Figure 6 a, b) for the mixture of  $\text{NH}_4$ -exchanged zeolite A and MgO, milled for 5 h and heated at 918 and 974 °C, exhibit the characteristic bands of forsterite.<sup>10</sup> The peaks at 1000, 842, 616, 505, 462 and 429  $\text{cm}^{-1}$  belong to forsterite since peaks at 892, 718, 530  $\text{cm}^{-1}$  are related to other phases. The peaks around 1000  $\text{cm}^{-1}$  are assigned to Si-O stretching modes and those around 500  $\text{cm}^{-1}$  to Mg-O stretching or Si-O bending modes.

FT-IR spectrum (Figure 6 c) for the mixture of  $\text{NH}_4$ -exchanged mordenite and MgO, milled for 10 h and heated at 855 °C, shows only the characteristic bands of crystalline forsterite.<sup>10,21,22</sup>

## CONCLUSIONS

Ball milling of the mixture of  $\text{NH}_4$ -exchanged zeolite A and MgO, and the mixture of  $\text{NH}_4$ -exchanged synthetic mordenite and MgO, resulted in the formation of an X-ray amorphous aluminosilicate and in a decrease of the particle size of crystalline MgO. By heating the mechanochemically treated mixtures at the temperatures of their phase transformation, which were observed as the temperatures of the exothermic peaks of the DSC curves, ceramic materials suitable for various applications were synthesized.

The mixture of  $\text{NH}_4$ -exchanged zeolite A and MgO, after milling for 5 h in a high energy ball mill and subsequent heating at 918 °C and 974 °C, transforms to forsterite powder and possibly small amounts of spinel and sapphirine.

The mixture of  $\text{NH}_4$ -exchanged synthetic mordenite and MgO, after grinding for 10 h in a high-energy ball mill and heating at 850 °C, transforms to a crystalline powder of forsterite and traces of enstatite. Using proper amounts of  $\text{NH}_4$ -exchanged synthetic mordenite and MgO as starting materials, pure forsterite may be synthesized by milling and subsequent heating of the mixture.

$\text{NH}_4$ -exchanged synthetic mordenite and MgO as starting materials were found to be more suitable for the synthesis of forsterite because of the lower content of Al ( $\text{Si}/\text{Al} \cong 5$ ) in the synthetic mordenite composition than in zeolite A ( $\text{Si}/\text{Al} \cong 1$ ). The Al content favours the synthesis of sapphirine or spinel.

The temperature of the observed transformations is much lower compared to the temperature required for the thermal transformation of mechanically untreated samples.

The findings of this paper offer interesting possibilities for the synthesis of pure forsterite or sapphirine using different ratios of  $\text{NH}_4$ -exchanged zeolites and MgO, previously mechanochemically treated in order to decrease the temperature of a possible phase transformation.

*Acknowledgement.* –The authors thank the Ministry of Science, Education and Sports of the Republic of Croatia for financial support.

## REFERENCES

1. L. Navias, *J. Am. Ceram. Soc.* **38** (1954) 329–351.
2. T. Ban, Y. Ohya, and Y. Takashushi, *J. Am. Ceram. Soc.* **82** (1999) 22–26.
3. (a) S. A. Boppart, G. J. Tearney, B. E. Bouma, J. F. Southern, M. E. Brezinski, and J. G. Fujimoto, *Proc. Natl. Acad. Sci. USA*, **94** (1997) 8405–8410; (b) F. Buchholz, L. Ringrose, P. O. Angrand, F. Rossi, and A. F. Stewart, *Nucleic Acid Res.* **24** (1996) 4256–4262.
4. B. R. Washburn, S. A. Diddams, N. R. Newbury, J. W. Nicholson, M. F. Yan, and C. G. Jorgensen, *Opt. Lett.* **29** (2004) 250–259.
5. A. Seas, V. Petričević, and R. R. Alfano, *Opt. Lett.* **18** (1993) 891–899.
6. G. W. Brindley and R. Hayami, *Philos. Mag.* **12** (1965) 505–514.
7. F. N. Cunha-Duncan and R. C. Bradt, *J. Am. Ceram. Soc.* **85** (2002) 2995–3003.
8. P. S. Devi, H. D. Gafney, V. Petričević, and R. R. Alfano, *J. Non-Cryst. Solids* **203** (1996) 78–83.
9. A. Kazakos, S. Komarneni, and R. Roy, *Mater. Lett.* **10** (9) (1990) 405–409.
10. D. G. Park, J. C. Duchamp, T. M. Duncan, and J. M. Burlitch, *Chem. Mater.* **6** (1994) 1990–1995.
11. S. Hashimoto and A. Yamaguchi, *J. Am. Ceram. Soc.* **78** (1995) 1989–1991.
12. R. W. Thompson and K. C. Franklin, *Verified Syntheses of Zeolitic Materials*, H. Robson (Ed.) Second Revised Edition, Elsevier Science, Amsterdam, 2001, p.179.
13. C. Kosanović, A. Čižmek, B. Subotić, I. Šmit, M. Stubičar, and A. Tonejc, *Zeolites* **15** (1995) 632–636.
14. C. Kosanović and B. Subotić, *Microporous Mater.* **12** (1997) 261–266.
15. *JCPDS International Centre for Diffraction Data*, Swarthmore, PA, 1996.
16. C. Kosanović, J. Bronić, B. Subotić, I. Šmit, M. Stubičar, A. Tonejc, and T. Yamamoto, *Zeolites* **13** (1993) 261–268.
17. E. M. Flanigen and H. Khatami, *Adv. Chem. Ser.* **101** (1971) 201–227.
18. H. Mimura and T. Kano, *T. Sci. Rep. RITU* **29A** (1980) 102–111.
19. Ch. Baerlocher, W. M. Meier, and D. H. Olson, *Atlas of Zeolite Framework Types*, 5th revised edition, Elsevier, Amsterdam, 2001.
20. K. C. Song, *Material Letters* **35** (1998) 290–296.
21. P. K. Lam, M. C. I. Yu, M. W. Lee, and S. K. Sharma, *Am. Mineral* **75** (1990) 109–119.
22. M. T. Tsai, *Mater. Res. Bull.* **37** (2002) 2213–2226.

**SAŽETAK****Sinteza forsterita iz zeolitnih prekursora****Cleo Kosanović, Nada Stubičar, Nenad Tomašić, Vladimir Bermanec, Mirko Stubičar i Hrvoje Ivanković**

Praškaste smjese od  $\text{NH}_4$ -zamićenog zeolita A i MgO te  $\text{NH}_4$ -zamićenog mordenita i MgO upotrijebljene su kao početni materijali u sintezi kristaliničnih keramičkih materijala. Intenzivno mljevenje kugličnim mlinom uporabljeno je radi amorfizacije  $\text{NH}_4$ -zamićenih zeolita i smanjenja veličine čestica MgO kao i radi bolje homogenizacije smjese. Grijanjem mljevenih uzoraka smjesa na temperaturama od 800–1000 °C u trajanju od 3 sata nastaje kristalinični forsterit ( $\text{Mg}_2\text{SiO}_4$ ) s minimalnim primjesama safirina ( $\text{Mg}_4\text{Al}_2\text{Si}_2\text{O}_{10}$ ) u prvom slučaju, odnosno kristalinični forsterit s tragovima enstatita ( $\text{MgSiO}_3$ ) u drugom slučaju.